Micropatterning of porous silicon Bragg reflectors with poly(ethylene glycol) to fabricate cell microarrays: Towards single cell sensing

Author:
Piya, R; Zhu, Y; Soeriyadi, AH; Silva, SM; Reece, PJ; Gooding, JJ

Publication details:
Biosensors and Bioelectronics
v. 127
Medium: Print-Electronic
pp. 229 - 235
0956-5663 (ISSN); 1873-4235 (ISSN)

Publication Date:
2019-02-15

Publisher DOI:
https://doi.org/10.1016/j.bios.2018.12.001

Micropatterning of Porous Silicon Bragg Reflectors With Poly(Ethylene Glycol) to Fabricate Cell Microarrays: Towards Single Cell Sensing

Ranjana Piya[a,b], Ying Zhu[a,b], Alexander H Soeriyadi[a], Saimon Moraes Silva[a], Peter J Reece[b], J Justin Gooding[a]

[a] School of Chemistry, Australian Centre for NanoMedicine and the ARC Centre of Excellence in Convergent Bio-Nano Science and Technology, The University of New South Wales, Sydney 2052, Australia.

[b] School of Physics, The University of New South Wales, Sydney 2052, Australia.

Abstract

The work presented here describes the development of optical label-free biosensor based on PSi Bragg reflector to study heterogeneity in single cells. Photolithographic patterning of poly(ethylene glycol) hydrogel with photoinitiator was employed on RGD peptide-modified PSi to create micropatterns with cell adhesive and cell repellent areas and J774 macrophage cells were incubated to form cell microarrays and single cell arrays. Moreover, cells on the microarrays were lysed osmotically with Milli-Q™ water and the infiltration of cell lysate into the porous matrix was monitored by measuring the red shift in the reflectivity. On average, the magnitude of red shift increased with the increase in the number of cells on the micropatterns. The red shift from the spots with single cells varied from spot to spot emphasizing the heterogeneous nature of the individual cells.

Keywords: porous silicon (PSi), cell patterning, cell lysis, label-free biosensing, poly(ethylene glycol (PEG) hydrogel

1. Introduction

The ability to position single or multiple cells at predefined location, also known as cell patterning, is an enabling technique in the study of fundamental aspects of cell biology such as cell-cell interactions, interaction of cells with their microenvironment and reaction of cells to external stimuli (Chen, Mrksich et al. 1998, Raghavan and Chen 2004, Lamponi, Di Canio et al. 2009, Yarmush and King 2009). Varieties of micropatterning techniques can be used for the generation of cell microarrays including spotting, photolithography, soft lithography and microfluidic devices (Zhang, Yan et al. 1999, Yap and Zhang 2007, Ceriotti, Buzanska et al. 2009). Among these techniques, micropatterning of photopolymerizable hydrogel using photolithography has received growing attention as it leads to the formation of precise 3D microstructures in a simple steps (Alexander Revzin and Curt Deister 2001, Yanagawa, Sugiura et al. 2016). One commonly used hydrogel in cell-based assays is poly(ethylene glycol) (PEG) hydrogel which is both nonfouling and biocompatible in the complex environments (Bjugstad, Redmond et al. 2008, Kim, Park et al. 2009, Bjugstad, Lampe et al. 2010). PEG with multi polymerizable end groups with a photoinitiator can form a cell or protein repelling hydrogel microstructures using a UV initiated free radical polymerization (Alexander Revzin and Curt Deister 2001, Ekblad, Bergström et al. 2008, Bae, Divan et al. 2010, Yeh, Venault et al. 2016). Such hydrogel microstructures can be exploited for cell patterning to study different aspects of cell biology including detection of cell secreted proteases (Shin, Liu et al. 2012, Son, Shin et al. 2013), cytokines (Zhu, Stybayeva et al. 2008, Zhu, Stybayeva et al. 2009, Yan and Revzin 2012), cell metabolites (Yan, Sun et al. 2009) and in capture and release of cells (Shin, Seo et al. 2011, Shin, You et al. 2014). PEG hydrogel patterning has been extensively conducted on flat surface like glass and silicon (Koh, Revzin et al. 2002, Revzin, Tompkins et al. 2003) and there are a few examples reported on porous substrate like nanoporous alumina (Lee, Kim et al. 2011). The advantage of using porous substrate is that the crosslinking of hydrogel can take place inside the porous matrix thus fixing the hydrogel micropatterns on the substrate firmly.

Porous silicon (PSi) is a versatile material for cell-based assays because of its biocompatibility (Chin, Collins et al. 2001, Low, Williams et al. 2006, Low, Voelcker et al. 2009), tunable optical properties and label-free optical biosensing (Schwartz, Derfus et al. 2006, Kilian, Lai et al. 2009, Guan, Magenau et al. 2011, Gupta, Mai et al. 2015). Moreover,

PSi is compatible with microfabrication technique which makes it an ideal platform for the formation of cell microarray. PSi can be fabricated by electrochemical etching of single crystalline silicon wafer and the optical properties can be tuned to reflect light at particular wavelengths. The sensing of PSi relies on the change in the position of the reflectivity peak in response to the addition or removal of materials with higher refractive index within or out of the pores. This mode of sensing makes PSi biosensors a potential label-free platform to study response of cells to external stimuli. Although there are various reports on micropatterning of PSi to promote selective attachment of cells on defined locations (Khung, Graney et al. 2006, Flavel, Sweetman et al. 2011, Sweetman, Shearer et al. 2011, Sweetman, Ronci et al. 2012, Dalilottojari, Delalat et al. 2016) so as to control the number of cells being studied, the potential of using PSi as a label-free optical biosensor to study cellular behaviour in cell microarrays has not been explored until now.

In this paper, we demonstrate the fabrication of single and multi-cell microarrays on PSi photonic structures using PEG hydrogel patterning. Also, we show that label-free optical sensing of single cells is possible using a cell lysis assay. To form cell microarrays, the PSi was first modified with the arginine-glycine-aspartic acid (RGD) peptide for the selective attachment of cells at defined positions. Then photolithographic PEG hydrogel patterning was performed using PEG precursor solution containing poly(ethylene glycol) diacrylate (PEGDA) and a photoinitiator (Irgacure 2959). The area of PSi with exposed RGD promotes the selective attachment point for the cells and the area with PEG hydrogel prevents the non-specific adsorption of the cells. Single or multi-cell microarrays were fabricated by incubating J774 macrophage cells on the patterned PSi surface. To demonstrate the utility of PSi as an optical biosensor in cell-based assays, optical reflectivity shift was monitored by lysing the cells osmotically on microarrays and letting the lysate to infiltrate into the porous matrix. Cell lysis was also confirmed by monitoring the leakage of stain from cells using a fluorescence microscope.

2. Materials and Methods

Details on chemicals, materials, apparatus and experiment procedures used in this work can be found in the Supplementary Information.

3. Results and Discussion

3.1 Surface Modification of PSi Bragg Reflector

To make PSi Bragg reflector surfaces amenable for the selective attachment of cells at precise locations, the freshly etched PSi Bragg reflector samples were first modified with surface chemistries requiring multiple modification steps as shown in Fig. S2a. Reflectivity spectra were collected after each modification step as a means to characterize the extent of molecular components being attached (Fig. S2b). When freshly etched PSi was hydrosilylated with 1,8-nonadiyne, Si-H bonds are replaced by robust Si-C bond and an organic monolayer was formed on PSi that prevents degradation of PSi surface in biological media. Since air was replaced by organic material, this results in an increase in average refractive index of PSi thus shifting the reflectivity peak position to longer wavelengths. Hydrosilylation of the dialkyne in this case resulted in a red shift of 41.5 nm (s = 1.0 nm, n = 35). Further modification of an alkyne-terminated PSi with a carboxyl group-terminated azide-containing EO_6 moieties *via* the archetypal click reaction, the Huisgen-1,3-dipolar cycloaddition reaction, resulted in another red shift of 7.4 nm (s = 1.0 nm, n = 35). This surface was further modified with the RGD peptide for the promotion of cell attachment after activating the carboxyl group with EDC/NHS chemistry. Since RGD is a short peptide, it yielded only a red shift of 1.8 nm (s = 1.0 nm, n = 35). Each surface modification step was also confirmed by XPS measurement on the surface (Fig. S3). XPS survey spectra and narrow scans of Si 2p and C 1s on the PSi Bragg reflector passivated with 1,8-nonadiyne are presented in Fig. S3a-c. Survey spectra shows the presence of expected elements Si, C and O on the surface. The peak at binding energy 285 eV (Fig. S3c) is indicative of carbon bound to carbon (C-C) which came from the functionalized alkyne layer. Survey spectra of the click functionalized PSi Bragg reflector shows the presence of an additional element N (Fig. S3d) that confirms the successful derivatization of alkyne functionalized PSi with azide containing EO_6 moieties (Ciampi, Böcking et al. 2007). Narrow scan of C 1s (Fig. S3f) showed some additional peaks at binding energies 286.8 eV indicative of C-O and 289.5 eV indicative of O-C=O. The high resolution N 1s data (Fig. S3e) shows two peaks centered at binding energies 400.5 eV and 402.0 eV which are indicative of the presence of chemically distinct nitrogen. This strongly suggests the formation of triazole moiety and successful modification of the PSi Bragg reflector surface with an azide species. An increase in the intensity of nitrogen peak at binding energy 400.5 eV (Fig. S3h) after the attachment of

peptide is attributed to the various nitrogen based peptide bonds in the peptide. Also, there is a significant increase in the intensity of O-C=O peak at 289.5 eV which is attributed to the carboxylic acid group in the peptide.

3.2 PEG Hydrogel Patterning on PSi Bragg Reflector

Scheme of PEG hydrogel patterning on RGD peptide-modified PSi Bragg reflector is shown in Fig. 1. In a typical experiment, a PEG precursor solution containing PEGDA and a photoinitiator Irgacure 2959 was dropped onto the RGD peptide-modified PSi and a glass coverslip was placed on top of PSi surface. The glass coverslip helped to homogeneously distribute the precursor solution throughout the surface and also prevent direct contact between a photomask and the substrate. Subsequently the PSi substrate was exposed with a UV light for 20 sec through a photomask in the MA6 mask aligner. PEG precursor solution behaved as a negative photoresist. When the precursor solution was exposed to UV light, the photoinitiator dissociated into very reactive free radicals that attacked the C=C of the monomer and initiated free radical polymerization. The precursor solution in the exposed region was thus crosslinked to form a hydrogel *via* radical chain polymerization (Fisher, Dean et al. 2001, Tan, Wang et al. 2008). The precursor solution from the unexposed regions was washed away with a water/ethanol mixture. Equation (i) demonstrates the PEG hydrogel formation process from the PEG precursor solution.

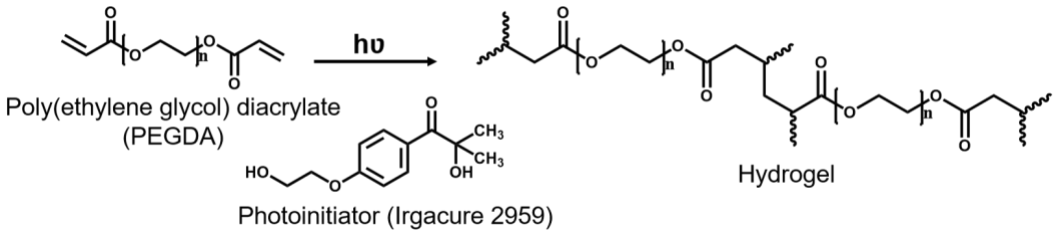

…… (i)

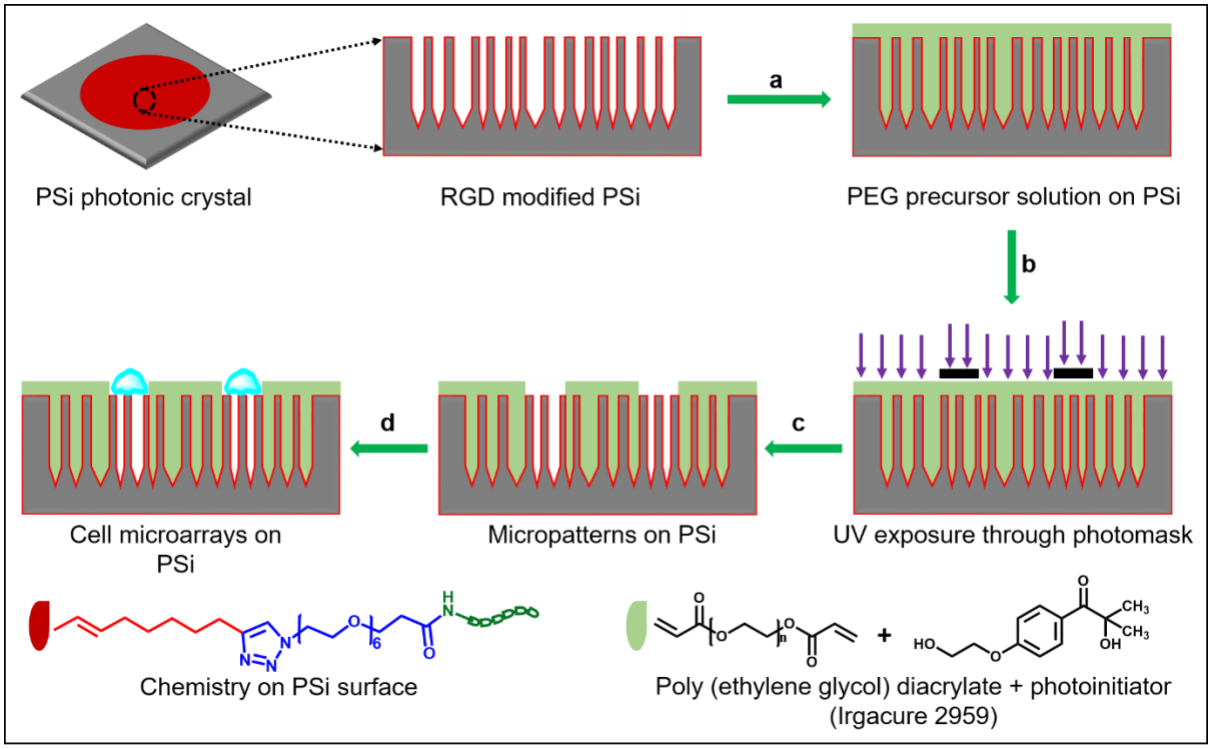

Fig. 1. Top view and cross-section scheme depicting photolithographic strategy to form PEG hydrogel micropatterns and cell microarray on PSi. **(a)** PEG precursor solution containing PEGDA and photoinitiator Irgacure 2959 was dropped on RGD peptide-modified PSi, **(b)** a glass coverslip was placed on top of PSi and the substrate was irradiated with UV light through a chrome-patterned photomask in a mask aligner, **(c)** exposed substrate was developed with water/ethanol mixture to wash unexposed PEG solution thus forming a micropatterns with exposed RGD peptide and **(d)** J774 macrophage cells were incubated with PEG hydrogel patterned PSi to form cell microarray.

3.3 Formation of Micropatterns and Cell Microarrays on PSi Bragg Reflector

Fig. 2a presents the bright field images of PEG hydrogel micropatterns formed on PSi with different feature size. The size of the micropatterns was controlled using a photomask with different pattern size. The pattern size of the mask and the actual pattern size formed on the surface can differ slightly depending upon slight over or underexposure of the substrate and also due to imperfect contact of the substrate and the mask. With the pattern size of 65 µm on the photomask, the actual pattern size formed on PSi was 65.1 µm (s = 1.8 µm, n = 100). Similarly with the pattern size of 50 µm and 20 µm on the mask, the actual pattern size formed was 49.6 µm (s = 2.1 µm, n = 100) and 20.1 µm (s = 1.5 µm, n = 100) respectively. Inside the circular regions RGD peptide is exposed which promotes the attachment of cells inside the circle (D'Souza, Ginsberg et al. 1991, Bellis 2011). RGD peptide is a ligand found in extracellular matrix proteins, namely fibronectin, which is recognized by integrin, cell surface

receptors (Ruoslahti and Pierschbacher 1987, Ruoslahti 1996). Outside the circle the antifouling PEG hydrogel restricts the attachment of cells (Ekblad, Bergström et al. 2008, Yeh, Venault et al. 2016). Thus the micropatterns formed on PSi with PEG hydrogel patterning have a potential for cell microarray formation.

For the formation of cell microarrays and single cell arrays, micropatterned PSi surfaces with different circle diameters were incubated with J774 macrophage cells for 6 h. Since the average size of J774 macrophage cells is 20 µm, we used 20 µm patterns for the fabrication of single cell arrays. After 6 h, surfaces were washed with growth media for 3 times to remove unbound or loosely bound cells on the surface. Cells were then stained with live/dead stain to check the viability of cells on the micropatterns. Fig. 2b shows the fluorescence images of cell microarray formed on PEG hydrogel micropatterns with different circle diameter. From the images, it is clear that cells adhered only onto the RGD peptide-modified area in PEG hydrogel patterned PSi. The green fluorescence is due to the enzymatic conversion of cell-permeant nonfluorescent calcein AM (live component in live/dead stain) to intensely fluorescent calcein in live cells. Ethidium homodimer-1 (dead component in live/dead stain) only enters the cells with damaged membranes and expresses very intense red fluorescence by interacting with nucleic acid. All the cells express an intense uniform green fluorescence indicates that the surfaces are cell compatible. Cell occupancy % was calculated for all different pattern size at the same cell seeding density ($1\times10_6$ cells/mL). For the bigger sizes of micropatterns (65 µm and 50 µm circle diameter), no empty spots were observed with 100% cell occupancy but in case of smaller micropatterns (20 µm circle diameter), cell occupancy % was less (59.4%). Among the total occupied spot in the 20 µm arrays, 65% of the elements were occupied with single cells.

Fig. 2c presents the actual number of cells adhered on the different patterns which clearly demonstrates that number of cells per pattern can be controlled by using different pattern size.

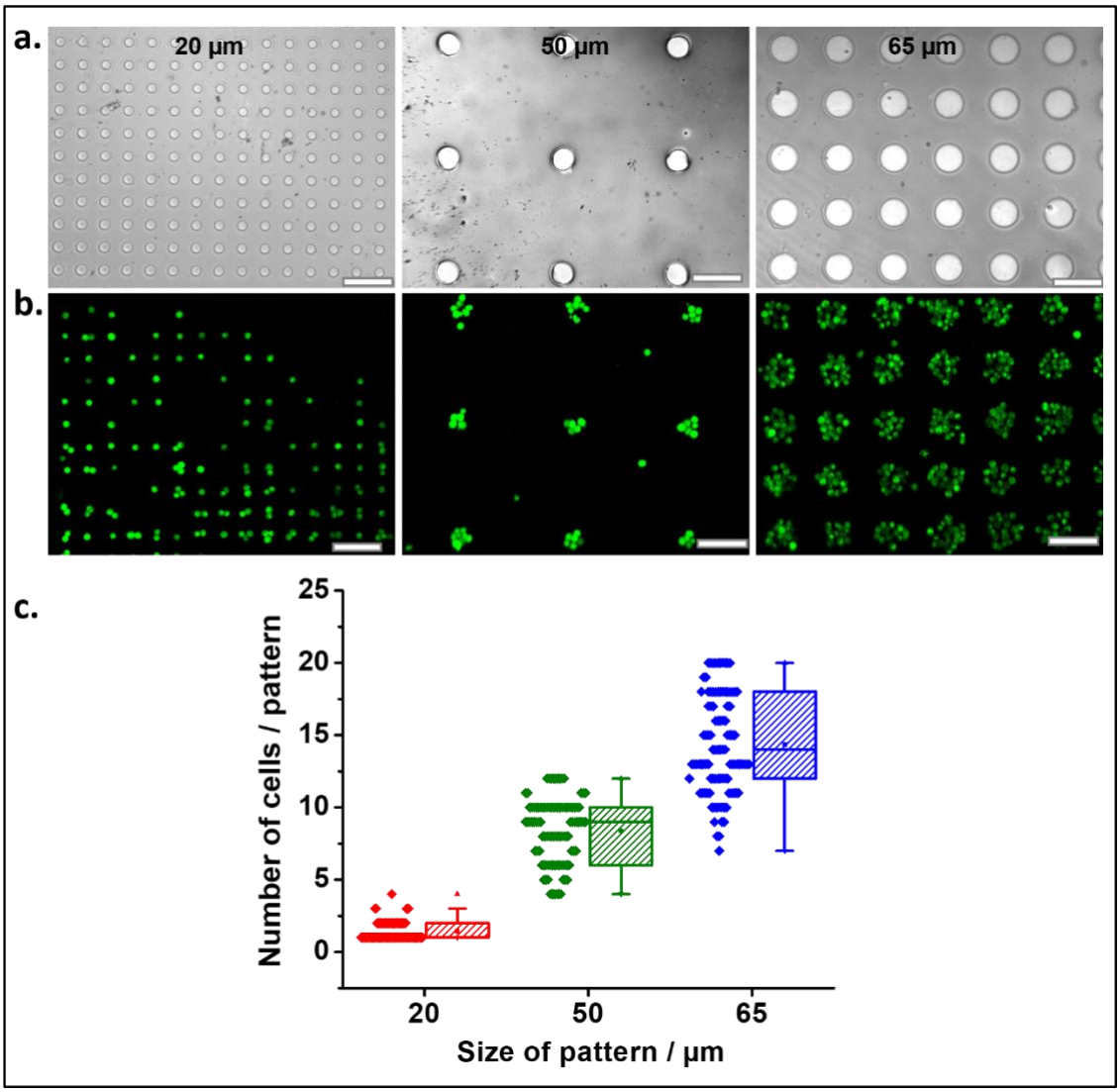

Fig. 2. (a) Bright field images of micropatterns formed on PSi with circle diameter 20 µm, 50 µm and 65 µm. **(b)** Fluorescence images of live/dead stained J774 macrophage cells on the corresponding micropatterns showing the formation of cell microarrays and single cell arrays and **(c)** the plot showing number of cells adhered on the spot with different diameter. The size of micropatterns can be controlled by using a photomask with different pattern size. The circular region has exposed RGD peptide for the attachment of cells whereas outside the circle has antifouling PEG hydrogel to prevent attachment of cells. The green fluorescence is due to the enzymatic conversion of cell-permeant nonfluorescent calcein AM (live component in live/dead stain) to intensely fluorescent calcein in live cells (scale bar 100 µm).

3.4 Cell Lysis on PSi Cell Microarrays

To demonstrate that we can use PSi Bragg reflectors as an optical biosensor in cell-based assays to analyze and discriminate between few and/or single cells, cells on the microarrays were lysed chemically using a lysis buffer Triton X-100 (0.1%) in PBS. When the cells are lysed, the cell membrane is ruptured and the released contents (cell lysate) infiltrate into the porous matrix. Since the lysate contains proteins, its infiltration into the porous matrix causes the increase in the average refractive index of PSi and the maxima of the reflectivity spectrum will red shift to longer wavelength. Before lysis, we first stained the cells with calcein AM. When the cells are lysed, there is a leakage of calcein from inside the cells due to the rupture of cell membrane (Fig. 3b) that leads to a decrease in fluorescence intensity. To confirm that cells are actually lysed with lysis buffer and to rule out the effect of photobleaching, we also measured the fluorescence intensity of cells exposed to PBS only (Fig. S4e). We found that the mean fluorescence intensity of cells exposed to lysis buffer dropped down to background in 6 minutes whereas the mean fluorescence intensity from spots containing non-lysed cells remained similar upon longer exposure to light when in PBS without Triton X-100 (Fig. S5).

After confirming that cells can be lysed on the micropatterns efficiently with a lysis buffer, we collected the reflectivity spectra from the micropatterns with cells + lysis buffer as well as no cells + lysis buffer. We found that the spots without cells exhibited a small red shift due to the surfactants present in the lysis buffer adsorbing to the pore walls and increasing the average refractive index of PSi in those spots. Such red shift from the spots without cells is undesirable especially when the goal is to detect very small changes in the amount of material released from cell into the pores. As such, to avoid any undesirable red shift caused by lysis buffer, we next explored the lysing of cells osmotically using Milli-Q™ water. Milli-Q™ water does not cause any undesirable red shifts. J774 macrophage cells were first incubated on PEG hydrogel patterned PSi surface for 6 hours in culture media. Then the culture media was replaced with Milli-Q™ water after removing the unbound cells by washing with culture media. When the culture media was replaced with Milli-Q™ water, there was an osmotic imbalance inside and outside the cells that caused excess water to move into the cells. As a result, the volume of the cell increased and reached the point where the volume exceeded the membrane's capacity, thus causing the membrane of the cell to rupture and their contents to

enter the pores of the PSi. Some remaining fragments of cells can be observed on the spots after cells burst (Fig. S6b). Due to contents of the cells infiltrating into the pores there is an increase in the average refractive index of PSi, thus causing the reflectivity peak position to red shift.

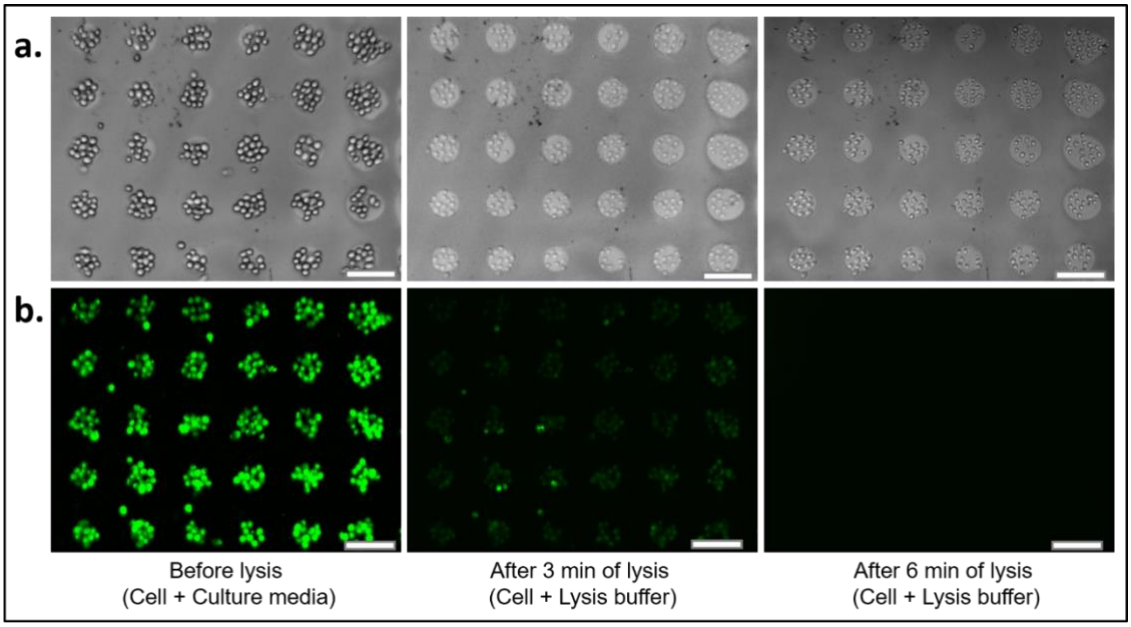

Fig. 3. (a) Bright field and **(b)** fluorescence images of J774 macrophage cells on 65 µm pattern before and after lysis. Cells were stained with calcein AM. When the cells are lysed, pores are created on the cell membrane thus causing the leakage of calcein from the cells. Thus the fluorescence intensity started to decrease due to the leakage of calcein. Cells are still on the micropatterns after lysis as can be seen from BF images. Scale bar 100 µm.

For the single cell lysis, the cells were cultured on the PEG hydrogel patterned PSi sample with circle diameter 20 µm. Reflectivity measurement was performed after 6 hours of Milli-Q™ water exposure. As a control, reflectivity was also collected from the sample with cells left in the culture media for 6 hours. Fig. 4a presents the plot of reflectivity peak shift for test (cells exposed to water) and control (cells left on culture media) samples. We observed that most of the spots in the sample with cells left in culture media for 6 hours showed almost no change in reflectivity or a minor blue shift presumably due to oxidation of the underlying silicon (Böcking, Kilian et al. 2008) whereas there is a noticeable red shift in the most of the spots of test sample exposed to Milli-Q™ water. This demonstrates that there is an infiltration of contents of cells after cell rupture onto the porous matrix which increased the average refractive index of PSi. Fig. 4b presents the statistical analysis of the optical shift based on Student's t-test. There is a significant difference in the red shift obtained from the spots with

lysed cells as compared to non-lysed cells. Fig. 4c is the plot of red shift obtained from the individual spots with different number of lysed cells as 20 µm patterns had one, two and three cells. It is obvious from the plot that there is a linear increase in the average red shift as the number of cells lysed on the spot increases. Most of the spots with lysed single cells have red shift ranging from 0.6-1.4 nm (n = 65). Fig. 4d is the histogram showing red shift obtained from individual spots upon which lysed single cells were located. As can clearly be observed from the histograms, there is significant heterogeneity in the response from single cells. At this stage it cannot be determined whether this variation in red shift is due to the heterogeneity within individual cells or from how the cells were ruptured such that there was variation in the amount of material that entered the pores.

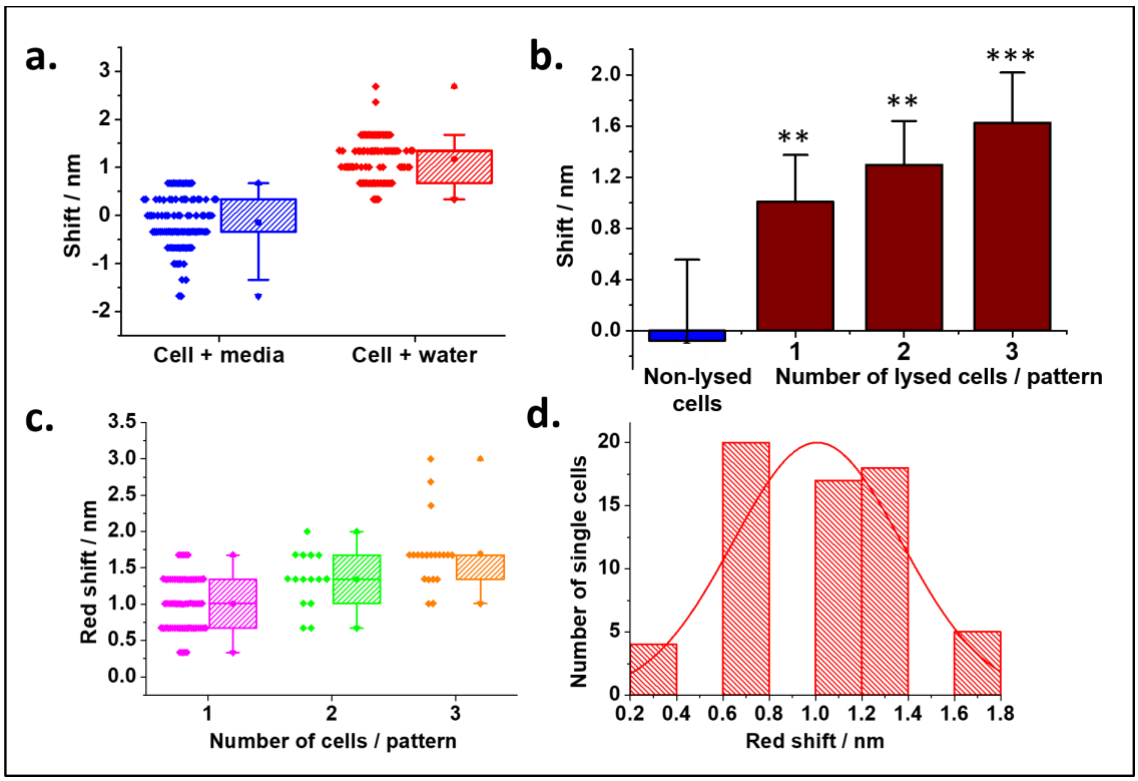

Fig. 4 (a) Plot of optical shifts obtained from the spots of test sample (cell + water) and control sample (cell + culture media) with 20 µm circle diameter. There is a noticeable red shift from the most of the spots of the sample exposed to water which is attributed to the infiltration of cellular contents into the porous matrix due to bursting of cells. On the other hand, most of the spots of the sample left in culture media have seen some blue shift. **(b)** Statistical analysis of red shift obtained from non-lysed cells (cell + media) and lysed cells (cell + water). Statistical significance was determined by Student's t-test. The bars with ** and *** indicate a statistical significance difference $p < 0.01$ and $p < 0.001$ respectively. Error bar is standard deviation. **(c)** Plot of optical shift obtained from individual spots with different number of cells (data analyzed from two different surfaces, n = 2) which shows that the average red

shift increases with an increase in the number of cells. **(d)** Histograms showing red shift from spots with single cells. Most of the spots with single cell have red shift ranging from 0.6-1.4 nm.

4. Conclusion

In summary, the work presented in this paper has demonstrated the potential of using PSi optical biosensor for label-free detection of biological events in the single cell-resolution. PEG hydrogel patterned PSi Bragg reflectors were shown to be compatible for the formation of cell microarrays and single cell arrays. In this proof of concept study the cells were adhered to individual elements of the array using the nonselective cell adhesive peptide RGD. However, we have previously shown on silicon surfaces that selectivity for one cell type over another can be achieved using antibodies (Guan, Magenau et al. 2014, Parker, Yang et al. 2018). It was also demonstrated that the number of cells on the spots can be controlled by fabricating the micropatterns of different diameter. To demonstrate the utility of PSi Bragg reflector as a label-free optical biosensor for monitoring single cell activities, cells on the micropatterns were lysed chemically and osmotically and the ingress of cell lysate into the porous matrix was monitored by measuring the red shift in the reflectivity spectrum. Significant difference in the red shift from the spots with lysed cells in comparison to non-lysed cells was observed which highlights the sensitivity of PSi optical biosensor in monitoring cellular activities at single-cell resolution. Cell lysis was also confirmed by measuring the decrease in mean fluorescence intensity from chemically-lysed cells.

The ability of monitoring response of single cells to specific stimuli has broad implications in studying cellular heterogeneity. At this stage the results demonstrate that there is sufficient material released from cells for PSi based cell arrays to explore cell heterogeneity. However, as stated above at this stage it is not 100% clear whether the heterogeneity in response is due to heterogeneity in the cell contents or how the cells ruptured. This can be more easily elucidated from exploring methods whether more controlled release of cell contents can be achieved. For example, with macrophage cells we have previously shown that matrix metalloproteinases can be stimulated to be released using lipopolysaccharide(Kilian, Lai et al. 2009). Such a strategy has yet to be explored at the single cells level but is more suitable to explore single cell heterogeneity, especially as the release of enzymes engenders the sensing system with an inbuilt amplification scheme which arises from the fact that each enzyme molecule can react with many substrate molecules inside the PSi pores. As such, the system

developed in the present study can be easily extended to study different biological events such as detecting enzymes, cytokines and metabolites released by single cells which could have great importance in studying cellular heterogeneity.

Acknowledgements

We acknowledge the generous financial support from the Australian Research Council through the Centre of Excellence in Convergent Bio-Nano Science and Technology (CE140100036) and for ARC Australian Laureate fellowship (FL150100060) for J.J.G.

References

Alexander Revzin, R. J. R., Vamsi K. Yadavalli, Won-Gun Koh, and D. D. H. Curt Deister, Michael B. Mellott, and Michael V. Pishko* (2001). "Fabrication of Poly(ethylene glycol) Hydrogel

Microstructures Using Photolithography." Langmuir **17**: 5440-5447.

Bae, M., R. Divan, K. J. Suthar, D. C. Mancini and R. A. Gemeinhart (2010). "Fabrication of Poly(ethylene glycol) Hydrogel Structures for Pharmaceutical Applications using Electron beam and Optical Lithography." J Vac Sci Technol B Microelectron Nanometer Struct Process Meas Phenom **28**(6): C6P24-C26P29.

Bellis, S. L. (2011). "Advantages of RGD peptides for directing cell association with biomaterials." Biomaterials **32**(18): 4205-4210.

Bjugstad, K. B., K. Lampe, D. S. Kern and M. Mahoney (2010). "Biocompatibility of poly(ethylene glycol)-based hydrogels in the brain: an analysis of the glial response across space and time." J Biomed Mater Res A **95**(1): 79-91.

Bjugstad, K. B., D. E. Redmond, Jr., K. J. Lampe, D. S. Kern, J. R. Sladek, Jr. and M. J. Mahoney (2008). "Biocompatibility of PEG-based hydrogels in primate brain." Cell Transplant **17**(4): 409-415.

Böcking, T., K. A. Kilian, K. Gaus and J. J. Gooding (2008). "Modifying Porous Silicon with Self-Assembled Monolayers for Biomedical Applications: The Influence of Surface Coverage on Stability and Biomolecule Coupling." Advanced Functional Materials **18**(23): 3827-3833.

Ceriotti, L., L. Buzanska, H. Rauscher, I. Mannelli, L. Sirghi, D. Gilliland, M. Hasiwa, F. Bretagnol, M. Zychowicz, A. Ruiz, S. Bremer, S. Coecke, P. Colpo and F. Rossi (2009). "Fabrication and characterization of protein arrays for stem cell patterning." Soft Matter **5**(7): 1406-1416.

Chen, C. S., M. Mrksich, S. Huang, G. M. Whitesides and D. E. Ingber (1998). "Micropatterned surfaces for control of cell shape, position, and function." Biotechnol Prog **14**(3): 356-363.

Chin, V., B. E. Collins, M. J. Sailor and S. N. Bhatia (2001). "Compatibility of Primary Hepatocytes with Oxidized Nanoporous Silicon." Advanced Materials **13**(24): 1877-1880.

Ciampi, S., T. Böcking, K. A. Kilian, M. James, J. B. Harper and J. J. Gooding (2007). "Functionalization of Acetylene-Terminated Monolayers on Si(100) Surfaces: A Click Chemistry Approach." Langmuir **23**(18): 9320-9329.

D'Souza, S. E., M. H. Ginsberg and E. F. Plow (1991). "Arginyl-glycyl-aspartic acid (RGD): a cell adhesion motif." Trends Biochem Sci **16**(7): 246-250.

Dalilottojari, A., B. Delalat, F. J. Harding, M. P. Cockshell, C. S. Bonder and N. H. Voelcker (2016). "Porous Silicon-Based Cell Microarrays: Optimizing Human Endothelial Cell-Material Surface Interactions and Bioactive Release." Biomacromolecules **17**(11): 3724-3731.

Ekblad, T., G. Bergström, T. Ederth, S. L. Conlan, R. Mutton, A. S. Clare, S. Wang, Y. Liu, Q. Zhao, F. D'Souza, G. T. Donnelly, P. R. Willemsen, M. E. Pettitt, M. E. Callow, J. A. Callow and B. Liedberg (2008). "Poly(ethylene glycol)-Containing Hydrogel Surfaces for Antifouling Applications in Marine and Freshwater Environments." Biomacromolecules **9**(10): 2775-2783.

Fisher, J. P., D. Dean, P. S. Engel and A. G. Mikos (2001). "PHOTOINITIATED POLYMERIZATION OF BIOMATERIALS." Annual Review of Materials Research **31**(1): 171-181.

Flavel, B. S., M. J. Sweetman, C. J. Shearer, J. G. Shapter and N. H. Voelcker (2011). "Micropatterned Arrays of Porous Silicon: Toward Sensory Biointerfaces." Acs Applied Materials & Interfaces **3**(7): 2463-2471.

Guan, B., A. Magenau, S. Ciampi, K. Gaus, P. J. Reece and J. J. Gooding (2014). "Antibody Modified Porous Silicon Microparticles for the Selective Capture of Cells." Bioconjugate Chemistry **25**(7): 1282-1289.

Guan, B., A. Magenau, K. A. Kilian, S. Ciampi, K. Gaus, P. J. Reece and J. J. Gooding (2011). "Mesoporous silicon photonic crystal microparticles: towards single-cell optical biosensors." Faraday Discussions **149**: 301-317.

Gupta, B., K. Mai, S. B. Lowe, D. Wakefield, N. Di Girolamo, K. Gaus, P. J. Reece and J. J. Gooding (2015). "Ultrasensitive and Specific Measurement of Protease Activity Using Functionalized Photonic Crystals." Analytical Chemistry **87**(19): 9946-9953.

Khung, Y.-L., S. D. Graney and N. H. Voelcker (2006). "Micropatterning of Porous Silicon Films by Direct Laser Writing." Biotechnology Progress **22**(5): 1388-1393.

Kilian, K. A., L. M. H. Lai, A. Magenau, S. Cartland, T. Boecking, N. Di Girolamo, M. Gal, K. Gaus and J. J. Gooding (2009). "Smart Tissue Culture: in Situ Monitoring of the Activity of Protease Enzymes Secreted from Live Cells Using Nanostructured Photonic Crystals." Nano Letters **9**(5): 2021-2025.

Kim, D.-N., J. Park and W.-G. Koh (2009). "Control of cell adhesion on poly(ethylene glycol) hydrogel surfaces using photochemical modification and micropatterning techniques." Journal of Industrial and Engineering Chemistry **15**(1): 124-128.

Koh, W.-G., A. Revzin and M. V. Pishko (2002). "Poly (ethylene glycol) hydrogel microstructures encapsulating living cells." Langmuir **18**(7): 2459-2462.

Lamponi, S., C. Di Canio and R. Barbucci (2009). "Heterotypic cell-cell interaction on micropatterned surfaces." Int J Artif Organs **32**(8): 507-516.

Lee, H. J., D. N. Kim, S. Park, Y. Lee and W. G. Koh (2011). "Micropatterning of a nanoporous alumina membrane with poly(ethylene glycol) hydrogel to create cellular micropatterns on nanotopographic substrates." Acta Biomater **7**(3): 1281-1289.

Low, S. P., N. H. Voelcker, L. T. Canham and K. A. Williams (2009). "The biocompatibility of porous silicon in tissues of the eye." Biomaterials **30**(15): 2873-2880.

Low, S. P., K. A. Williams, L. T. Canham and N. H. Voelcker (2006). "Evaluation of mammalian cell adhesion on surface-modified porous silicon." Biomaterials **27**(26): 4538-4546.

Parker, S. G., Y. Yang, S. Ciampi, B. Gupta, K. Kimpton, F. M. Mansfeld, M. Kavallaris, K. Gaus and J. J. Gooding (2018). "A photoelectrochemical platform for the capture and release of rare single cells." Nature Communications **9** 2288.

Raghavan, S. and C. S. Chen (2004). "Micropatterned Environments in Cell Biology." Advanced Materials **16**(15): 1303-1313.

Revzin, A., R. G. Tompkins and M. Toner (2003). "Surface Engineering with Poly(ethylene glycol) Photolithography to Create High-Density Cell Arrays on Glass." Langmuir **19**(23): 9855-9862.

Ruoslahti, E. (1996). "RGD and other recognition sequences for integrins." Annu Rev Cell Dev Biol **12**: 697-715.

Ruoslahti, E. and M. Pierschbacher (1987). "New perspectives in cell adhesion: RGD and integrins." Science **238**(4826): 491-497.

Schwartz, M. P., A. M. Derfus, S. D. Alvarez, S. N. Bhatia and M. J. Sailor (2006). "The smart petri dish: A nanostructured photonic crystal for real-time monitoring of living cells." Langmuir **22**(16): 7084-7090.

Shin, D.-S., Y. Liu, Y. Gao, T. Kwa, Z. Matharu and A. Revzin (2012). "Micropatterned Surfaces Functionalized with Electroactive Peptides for Detecting Protease Release from Cells." Analytical Chemistry **85**(1): 220-227.

Shin, D.-S., J. H. Seo, J. L. Sutcliffe and A. Revzin (2011). "Photolabile micropatterned surfaces for cell capture and release." Chemical Communications **47**(43): 11942-11944.

Shin, D.-S., J. You, A. Rahimian, T. Vu, C. Siltanen, A. Ehsanipour, G. Stybayeva, J. Sutcliffe and A. Revzin (2014). "Photodegradable Hydrogels for Capture, Detection, and Release of Live Cells." Angewandte Chemie (International ed. in English) **53**(31): 8221-8224.

Son, K. J., D. S. Shin, T. Kwa, Y. Gao and A. Revzin (2013). "Micropatterned sensing hydrogels integrated with reconfigurable microfluidics for detecting protease release from cells." Anal Chem **85**(24): 11893-11901.

Sweetman, M. J., M. Ronci, S. R. Ghaemi, J. E. Craig and N. H. Voelcker (2012). "Porous Silicon Films Micropatterned with Bioelements as Supports for Mammalian Cells." Advanced Functional Materials **22**(6): 1158-1166.

Sweetman, M. J., C. J. Shearer, J. G. Shapter and N. H. Voelcker (2011). "Dual Silane Surface Functionalization for the Selective Attachment of Human Neuronal Cells to Porous Silicon." Langmuir **27**(15): 9497-9503.

Tan, G., Y. Wang, J. Li and S. Zhang (2008). "Synthesis and Characterization of Injectable Photocrosslinking Poly (ethylene glycol) Diacrylate based Hydrogels." Polymer Bulletin **61**(1): 91-98.

Yan, J. and A. Revzin (2012). Micropatterned Biosensing Surfaces for Detection of Cell-Secreted Inflammatory Signals. Biosensors and Molecular Technologies for Cancer Diagnostics, Taylor & Francis**:** 389-404.

Yan, J., Y. Sun, H. Zhu, L. Marcu and A. Revzin (2009). "Enzyme-containing hydrogel micropatterns serving a dual purpose of cell sequestration and metabolite detection." Biosensors and Bioelectronics **24**(8): 2604-2610.

Yanagawa, F., S. Sugiura and T. Kanamori (2016). "Hydrogel microfabrication technology toward three dimensional tissue engineering." Regenerative Therapy **3**: 45-57.

Yap, F. L. and Y. Zhang (2007). "Protein and cell micropatterning and its integration with micro/nanoparticles assembly." Biosensors and Bioelectronics **22**(6): 775-788.

Yarmush, M. L. and K. R. King (2009). "Living-Cell Microarrays." Annual review of biomedical engineering **11**: 235-257.

Yeh, C.-C., A. Venault and Y. Chang (2016). "Structural effect of poly(ethylene glycol) segmental length on biofouling and hemocompatibility." Polym J **48**(4): 551-558.

Zhang, S., L. Yan, M. Altman, M. Lassle, H. Nugent, F. Frankel, D. A. Lauffenburger, G. M. Whitesides and A. Rich (1999). "Biological surface engineering: a simple system for cell pattern formation." Biomaterials **20**(13): 1213-1220.

Zhu, H., G. Stybayeva, M. Macal, E. Ramanculov, M. D. George, S. Dandekar and A. Revzin (2008). "A microdevice for multiplexed detection of T-cell-secreted cytokines." Lab on a Chip **8**(12): 2197-2205.

Zhu, H., G. Stybayeva, J. Silangcruz, J. Yan, E. Ramanculov, D. Satya, M. George and A. Revzin (2009). "Detecting Cytokine Release from Single Human T-cells." Analytical chemistry **81**(19): 8150-8156.